Dig Dis Sci (2018) 63:81–91
https://doi.org/10.1007/s10620-017-4801-x

ORIGINAL ARTICLE

Propofol Does Not Reduce Pyroptosis of Enterocytes and Intestinal Epithelial Injury After Lipopolysaccharide Challenge

Xu-Yu Zhang[1] · Xi Chen[1] · Hu-Fei Zhang[1] · Su Guan[2] · Shi-Hong Wen[1] · Wen-Qi Huang[1] · Zi-Meng Liu[3]

Received: 9 September 2017 / Accepted: 10 October 2017 / Published online: 23 October 2017

Abstract

Background To date, mechanisms of sepsis-induced intestinal epithelial injury are not well known. P2X7 receptor (P2X7R) regulates pyroptosis of lymphocytes, and propofol is usually used for sedation in septic patients.

Aims We aimed to determine the occurrence of enterocyte pyroptosis mediated by P2X7R and to explore the effects of propofol on pyroptosis and intestinal epithelial injury after lipopolysaccharide (LPS) challenge.

Methods A novel regimen of LPS challenge was applied in vitro and in vivo. Inhibitors of P2X7R (A438079) and NLRP3 inflammasome (MCC950), and different doses of propofol were administered. The caspase-1 expression, caspase-3 expression, caspase-11 expression, P2X7R expression and NLRP3 expression, extracellular ATP concentration and YO-PRO-1 uptake, and cytotoxicity and HMGB1 concentration were detected to evaluate enterocyte pyroptosis in cultured cells and intestinal epithelial tissues. Chiu's score, diamine oxidase and villus length were used to evaluate intestinal epithelial injury. Moreover, survival analysis was performed.

Results LPS challenge activated caspase-11 expression and P2X7R expression, enhanced ATP concentration and YO-PRO-1 uptake, and led to increased cytotoxicity and HMGB1 concentration. Subsequently, LPS resulted in intestinal epithelial damage, as evidenced by increased levels of Chiu's score and diamine oxidase, and shorter villus length and high mortality of animals. A438079, but not MCC950, significantly relieved LPS-induced enterocyte pyroptosis and intestinal epithelial injury. Importantly, propofol did not confer the protective effects on enterocyte pyroptosis and intestinal epithelia although it markedly decreased P2X7R expression.

Conclusion LPS attack leads to activation of caspase-11/P2X7R and pyroptosis of enterocytes. Propofol does not reduce LPS-induced pyroptosis and intestinal epithelial injury, although it inhibits P2X7R upregulation.

Keywords Sepsis · Lipopolysaccharide · P2X7 receptor · Enterocytes · Caspase

Xu-Yu Zhang and Xi Chen contributed equally to this work.

✉ Zi-Meng Liu
sumslzm@163.com

Xu-Yu Zhang
sumsxyz@163.com

Xi Chen
604046054@qq.com

Hu-Fei Zhang
zhanghufei_fly@163.com

Su Guan
guansu@scut.edu.cn

Shi-Hong Wen
wenshihong2006@aliyun.com

Wen-Qi Huang
sumshwq@gmail.com

[1] Department of Anesthesiology, The First Affiliated Hospital, Sun Yat-sen University, Guangzhou 510089, China

[2] School of Biology and Biological Engineering, South China University of Technology, Guangzhou 510006, China

[3] Surgical Intensive Care Unit, The First Affiliated Hospital, Sun Yat-sen University No. 58, Zhongshan 2nd Road, Guangzhou 510080, China

Introduction

The newest definition of sepsis is a "life-threatening organ dysfunction cause by a dysregulated host response to infection." The "Surviving Sepsis Campaign" has developed evidence-based guidelines for the recognition and management of severe sepsis and septic shock [1]. However, to date, sepsis remains a leading cause of death in hospital and consumes massive medical resources [1, 2]. The intact intestinal barrier plays an important protective role in sepsis [3]. Enterocyte death caused by sepsis results in epithelial barrier dysfunction [4, 5] and subsequently causes multiple organ dysfunction syndrome and poor clinical outcomes [6, 7]. It has been demonstrated that intestinal epithelial apoptosis largely increases in septic experiments [8, 9]. So far, however, mechanisms of enterocyte damage during sepsis have not been well elucidated.

Pyroptosis, a distinct form of programmed cell death, is mediated by caspase-1 (canonical pathway) or caspase-11 (noncanonical pathway) [10]. Pyroptosis operates to defense against microbial infections, but aberrant activation of pyroptosis may contribute to the development of sepsis [11]. P2X7 purinergic receptor (P2X7R) is a ATP-gated ion channel. LPS or ATP stimulation via P2X7R leads to the opening of a larger pore that allows the uptake of organic molecules, and subsequently induces the destruction of cells [10]. Growing evidences demonstrated that P2X7R played a critical role in the induction of pyroptosis mediated by caspase-1 and caspase-11, and the absence of P2X7R decreased immune cell death and animal's mortality after cecal ligation and puncture (CLP) and lipopolysaccharide (LPS) attack [10, 12]. Importantly, a recent literature showed that P2X7R expressed in intestinal epithelial cells [13]. Propofol, a common hypnotic agent in general anesthesia and critical illness, offered a protection against apoptosis of enterocytes following LPS attack and burn injury [14, 15]. However, few studies have explored the effect of propofol on potential pyroptosis of enterocytes during sepsis. Interestingly, propofol could inhibit P2X7R upregulation induced by cardiac arrest in neurons [16]. Therefore, we hypothesized that, in sepsis, LPS may induce enterocyte pyroptosis, and propofol may attenuate pyroptosis through inhibiting P2X7R expression.

Taken together, the aim of this study is to verify the occurrence of enterocyte pyroptosis and to investigate the effect of propofol on P2X7R-associated pyroptosis and intestinal epithelial injury after LPS challenge.

Methods

Cell Lines and Animals

The rat intestinal epithelial cell line (IEC-6, CRL-1592) was purchased from the American Type Culture Collection (ATCC, Rockefeller, MD, USA). IEC-6 cells were cultured in Dulbecco's modified Eagle's medium (DMEM) containing 10% (v/v) fetal bovine serum and 1% bovine insulin, 100 U/mL of penicillin/streptomycin (Sigma-Aldrich, St. Louis, MO, USA), and were maintained at 37 °C in a humidified 5% CO_2 incubator.

The animal experiment (protocol number 17-#2-28) was approved by the Animal Care Committee of Sun Yat-sen University and was performed in accordance with National Institutes of Health guidelines for the experimental animals. Eight- to 10-week-old SPF male C57BL/6 mice (23.5–29.6 g) were purchased from Laboratory Animal Center of Sun Yat-sen University. The mice were housed in individual cages in a temperature-controlled room with alternating 12-h light–dark cycles and were acclimated for 1 week before protocol entry.

LPS Challenge

According to the novel literatures [10, 17], LPS stimulation was used in vitro and in vivo.

In vitro, IEC-6 cells were seeded at 5×10^4 cells per well onto 96-well plates and allowed to grow to 90% confluence. DMEM was replaced with Opti-MEM (Sigma-Aldrich, St. Louis, MO, USA), and the cells were treated with LPS from 50 ng/mL *E. coli* O111:B4 (Sigma-Aldrich) in Opti-MEM overnight. For LPS transfection, 75 ng of LPS (S. Minnesota RE595, Sigma-Aldrich) and 375 ng DOTAP (Sigma-Aldrich) were suspended in 2 µl of Opti-MEM for 5 min, and then suspensions were mixed and incubated for 30 min at room temperature. Reaction volumes were brought up to 100 µL with Opti-MEM and then added to IEC-6 cells and centrifuged for 5 min at $200 \times g$.

In vivo, LPS from *E. coli* O111:B4 (Sigma-Aldrich) was dissolved in PBS. C57BL/6 mice were primed with 400 µg/kg LPS by intraperitoneal injections for 6 h. Then the mice were challenged with 10 mg/kg of intraperitoneal LPS.

Experimental Protocol

The cultured cells and mice were randomly allocated into six groups, respectively. In the experiments, all the study-drugs were dissolved and diluted by normal saline (NS). Equivalent volume of solution was added to every culture

medium, and each mouse received equivalent volume of intraperitoneal injection.

1. Group C (control): The IEC-6 cells and mice were not treated with LPS. Pure NS was used in this group.
2. Group L (LPS): LPS were dissolved and diluted by NS. Sepsis model was produced by LPS in the IEC-6 cells and mice according to the above-mentioned protocol.
3. Group A (A438079): A438079, a specific competitive P2X7R antagonist, was used to explore the role of P2X7R in intestinal epithelial pyroptosis after LPS attack. In vitro, 5 mM A438079 (Santa Cruz Biotechnology, Santa Cruz, CA, USA) dissolved in NS was added to the cultured cells 1 h before LPS transfection. In vivo, 80 mg/kg A438079 dissolved in NS was intraperitoneally administered soon after secondary LPS injection.
4. Group M (MCC950): NLRP3 inflammasome plays a critical role in the canonical induction of pyroptosis [10]. Thus, MCC950, a specific inhibitor of NLRP3, was used to explore the role of NLRP3 in intestinal epithelial pyroptosis after LPS attack. In vitro, 50 μM MCC950 (MedChem Express, Shanghai, China) dissolved in NS was given 1 h before LPS transfection. In vivo, 50 mg/kg MCC950 dissolved in NS was intraperitoneally administered soon after secondary LPS injection.
5. Group P (propofol): In vitro, 50, 250 and 500 μM propofol (Diprivan 1%, Astra Zeneca, Caponago, Italy) diluted by NS was added to the IEC-6 cells 1 h before LPS transfection. In vivo, 50, 75 and 100 mg/kg propofol was attempted to use in our preliminary experiments, whereas 75 and 100 mg/kg propofol frequently caused severe respiratory and cardiac depression of mice (data not shown). Thus, 50 mg/kg propofol diluted by NS was administered intraperitoneally to mice immediately after secondary LPS injection in the following experiments.
6. Group I (intralipid): Intralipid 10% (Baxter Healthcare, Chicago, IL, USA) is the vehicle solution of propofol. In vitro, intralipid diluted by NS was used to incubate with the IEC-6 cells 1 h before LPS transfection. In vivo, the mice received equivalent volume of intralipid diluted by NS after secondary LPS injection.

At 2 h after LPS transfection, the cultured IEC-6 cells were collected and examined. Furthermore, at 24 h after first injection with LPS, the mice were euthanized and biological samples were harvested as we previously described [18]. Briefly, blood was collected via cardiac puncture; a ~ 0.5-cm segment of intestine was cut next to terminal ileum for immunohistochemical analysis. Another segment of intestine (~ 10 cm) was obtained from 5 cm to terminal ileum, and the intestinal epithelial tissues were scraped off gently and preserved in liquid nitrogen.

Western Blot

Proteins from IEC-6 cells and intestinal samples were extracted by using a total protein extraction kit (Biochain, Los Angeles, CA, USA) and were quantified by using the BCA protein assay kit (Pierce Biotechnology Inc., Rockford, IL, USA). Proteins were subjected to SDS-PAGE and then were electrophoretically transferred to nitrocellulose membrane. Membranes were blocked with a solution composed of 5% fat dry milk in Tween-containing Tris-buffered saline for 2 h at room temperature. The blocked membranes were subsequently incubated with antibodies of rat (in vitro) or mouse (in vivo) against caspase-1, caspase-3, caspase-11, NLRP3, P2X7R and GAPDH overnight at 4 °C. The antibodies were purchased from Santa Cruz Biotechnology (Santa Cruz, CA, USA), Adipogen Corporation (San Diego, CA, USA) and Novus Biologicals (Littleton, CO, USA). The membranes were then washed and incubated with the secondary antibodies (Santa Cruz Biotechnology) directed at the primary antibody for 1 h at room temperature. The band density was analyzed densitometrically and normalized with the GAPDH protein. The data were calculated and presented as percentage of the group L.

Cytotoxicity Assay

Pyroptosis of cultured IEC-6 cells was assessed by cytotoxicity assay [10, 19]. Briefly, cytotoxicity was detected by using the CytoTox 96® Non-Radioactive Cytotoxicity Assay kit (Promega Corporation, Madison, WI, USA) according to manufacturer's instructions. The cytotoxicity was normalized to total lactate dehydrogenase activity in cell lysates.

ATP Measurement

At 2 h after LPS transfection, culture medium in each well was centrifuged at 1500 rpm for 1 min, and 10 mL of the supernatant was collected for ATP measurement. The extracellular ATP concentration was measured by using ATPlite Luminescence ATP Detection Assay System (PerkinElmer, Waltham, MA, USA) according to manufacturer's manual [20].

YO-PRO-1 Uptake Assay

Activation of P2X7R was assessed by YO-PRO-1 uptake [10]. IEC-6 cells treated with various interventions were stained with 1 μM YO-PRO-1 iodide (Thermo Scientific,

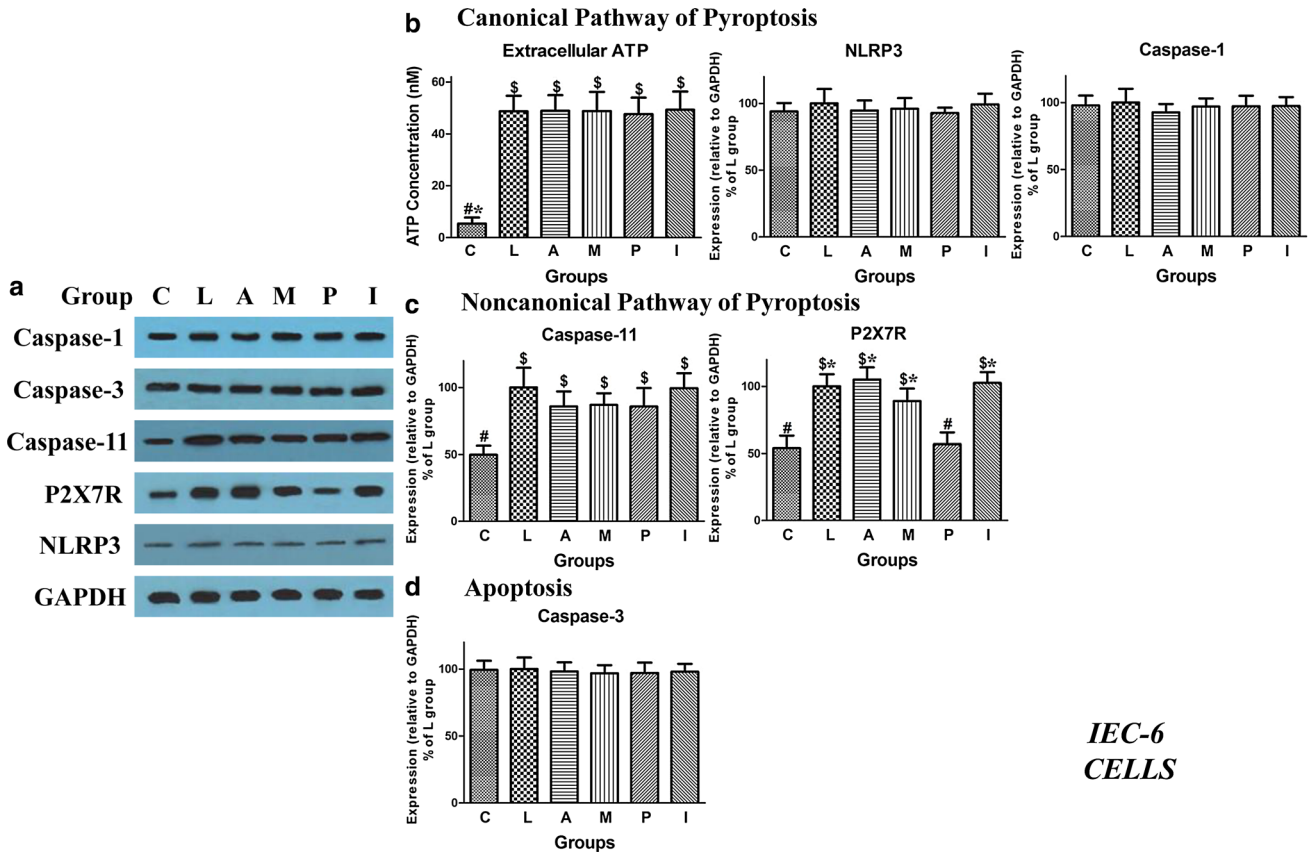

Fig. 1 Changes in the expression of various molecules and the concentration of extracellular ATP in cultured IEC-6 cells. **a** The expression of various molecules in pyroptotic and apoptotic pathways was detected by western blot. Representative bands from densitometric analysis in experimental groups were presented. **b** The ATP concentration, NLRP3 expression and caspase-1 expression in canonical pyroptosis were analyzed and presented. **c** The caspase-1 expression and P2X7R expression in noncanonical pyroptosis were analyzed and presented. **d** The caspase-3, a biomarker of apoptosis, expression was analyzed and presented. Data were expressed as mean ± SD, $n = 5$. Results were compared by ANOVA with Tukey posttest. $^{\$}P < 0.01$ versus the C group; $^{*}P < 0.01$ versus the *P* group; $^{\#}P < 0.01$ versus the L group. P2X7R, P2X7 receptor; C, control group; L, lipopolysaccharide group; A, A438079 group (a competitive antagonist of P2X7 receptor); M, MCC950 group (an inhibitor of NLRP3); P, propofol group (a common hypnotic, 50 μM); I, intralipid group (vehicle of propofol)

Hudson, NH, USA) for 15 min at room temperature, washed with PBS and then fixed by 4% paraformaldehyde solution in PBS for 20 min. Finally, nuclear staining was accomplished with 0.5 μg/mL 4′,6-diamidino-2-phenylindole (DAPI). The analysis was performed by using a fluorescence microscope (Nikon, Tokyo, Japan). In each well, YO-PRO-1 stained cells were counted in three randomly selected fields and presented as the percentage of the total number of cells identified by DAPI staining in the same field. The data were calculated and averaged to determine the opening of P2X7R-associated pore.

Enzyme-Linked Immunosorbent Assay (ELISA)

Pyroptosis mediated by Caspase-1 leads to the release of interleukin (IL)-1β and IL-18. The concentrations of IL-1β and IL-18 in cell culture supernatants were measured by ELISA kits (CUSABIO, Wuhan, China) according to the manufacturer's manual. High-mobility group box-1 protein (HMGB1) is a signal of necrotic and pyroptotic cells [21], and diamine oxidase (DAO) is an indicator of the integrity and functional mass of the intestinal epithelia [22]. Intestinal epithelial tissues were homogenized on ice with NS and centrifuged for 15 min at 4000×*g*, and then the supernatants were collected. The amounts of HMGB1 and DAO were measured by ELISA kit (Shino-Test Corporation, Kanagawa, Japan and CUSABIO, Wuhan, China) in the supernatants, respectively.

Immunohistochemical Analysis

The ∼ 0.5-cm intestinal segment was fixed and sectioned, and then stained with hematoxylin–eosin. Two independent pathologists assessed the histological damage by using Chiu's score, as previously described [7].

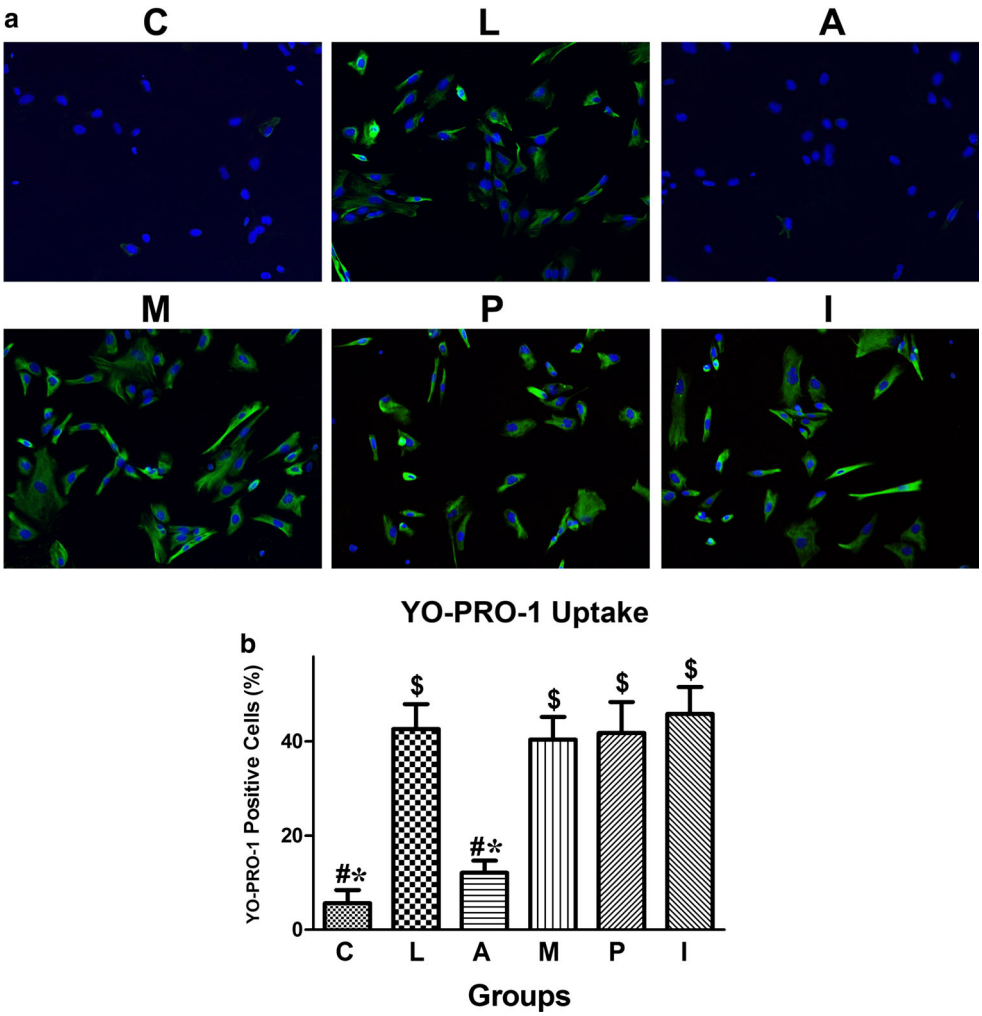

Fig. 2 Changes in YO-PRO-1 uptake in cultured IEC-6 cells. The opening of larger pores on cell membrane allows the passage of fluorescent dyes. Thus, we assessed the opening of P2X7R-associated pores by measuring the uptake of YO-PRO-1. The cultured cells were stained with YO-PRO-1 (green) and DAPI (blue) counterstained nuclei. **a** The stained cells in experimental groups were examined by fluorescence microscope. Representative fluorescence microscopic images (×200) of YO-PRO-1 in experimental groups were shown. **b** The percentage of YO-PRO-1 positive cells was analyzed and presented. Data were expressed as mean ± SD, $n = 5$. Results were compared by ANOVA with Tukey posttest. $^{\$}P < 0.01$ versus the C group; $^{*}P < 0.01$ versus the P group; $^{\#}P < 0.01$ versus the L group. C, control group; L, lipopolysaccharide group; A, A438079 group (a competitive antagonist of P2X7 receptor); M, MCC950 group (an inhibitor of NLRP3); P, propofol group (a common hypnotic, 50 μM); I, intralipid group (vehicle of propofol)

Moreover, according to the similar literature [23, 24], villus length was used to assess the histological injury of intestine after sepsis. Villus length was determined by measuring the distance from the crypt neck to the villus tip. A minimum of 10 well-oriented villi from each section were measured.

Survival Analysis

The survival analysis was evaluated in independent mice as we previously described [18]. Briefly, the mice treated with the various interventions (indicated in "Experimental Protocol") were transferred to their cages and monitored via video recording for 72 h.

Statistical Analysis

Statistics were analyzed with SPSS 18.0 software (SPSS Inc., Chicago, IL, USA). Survival time was expressed as median (interquartile). The results of survival time after secondary LPS attack were compared by Kaplan–Meier log-rank test and Fisher's exact test. The other data were expressed as mean ± standard deviation (SD) and were compared through one-way ANOVA with Tukey posttest. $P < 0.05$ in two-tailed testing was considered statistically significant.

Results

LPS Challenge Induced Activation of Caspase-11, Upregulation and Opening of P2X7R, and Pyroptosis of Enterocyte in Cultured Cells

In cultured IEC-6 cells, the expression of various molecules in canonical and noncanonical pathway of pyroptosis was measured by using western blot analysis (Fig. 1a). After LPS attack, in canonical pathway of pyroptosis, the extracellular ATP concentration elevated in the group L ($P < 0.001$ vs. group C), whereas the expression of NLRP3 and caspase-1 was not significantly different between group L and group C (both $P > 0.05$; Fig. 1b). As shown in

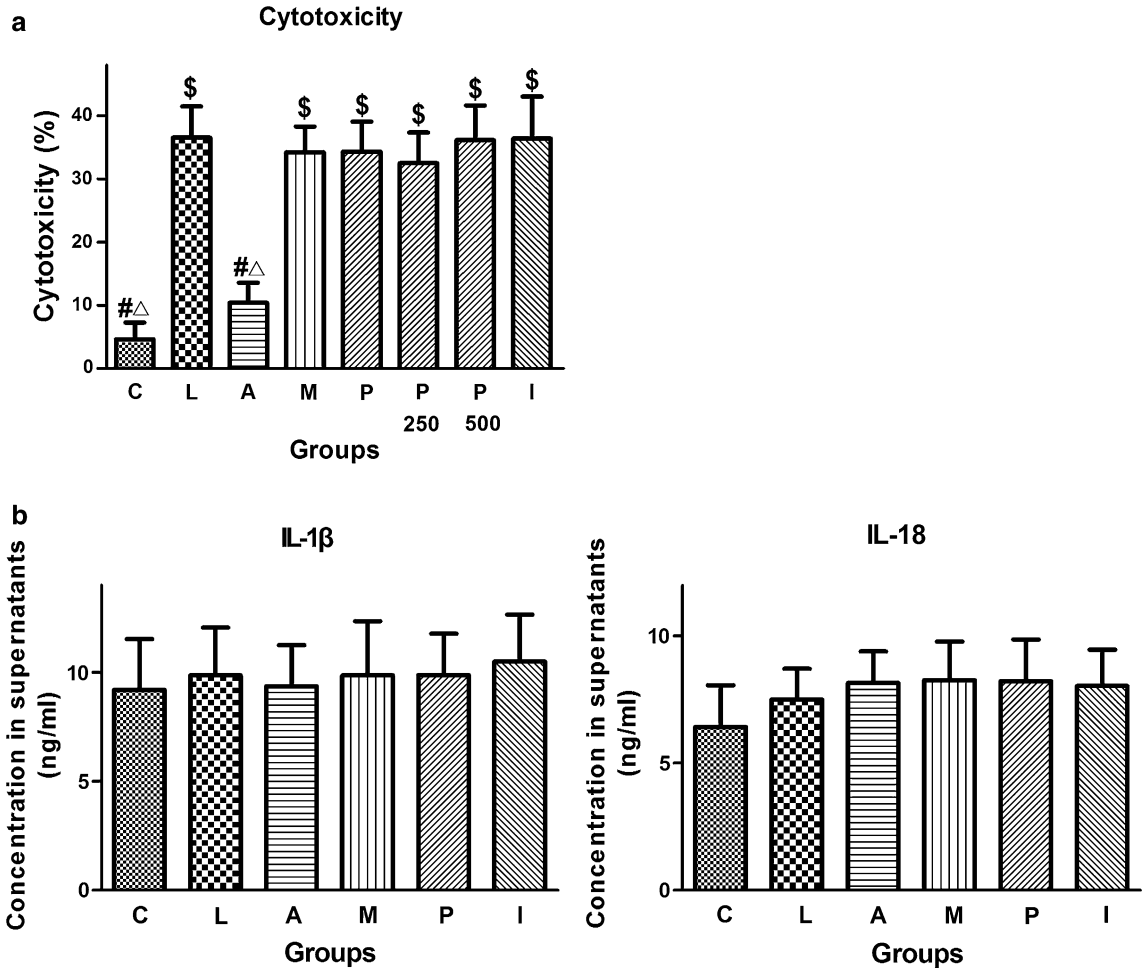

Fig. 3 Changes in cytotoxicity and IL-1β, IL-18 in cultured IEC-6 cells. **a** Cytotoxicity is a specific biomarker of pyroptosis in cultured cells. Cytotoxicity was analyzed by a CytoTox kit and presented. **b** IL-1β and IL-18 are canonical pyroptosis-associated cytokines. Analysis of IL-1β and IL-18 concentration in culture media was presented. Data were expressed as mean ± SD, $n = 5$–6. Results were compared by ANOVA with Tukey posttest. $^{\$}P < 0.01$ versus the C group; $^{\#}P < 0.01$ versus the L group; $^{\triangle}P < 0.01$ versus the P, P250 and P500, group. C, control group; L, lipopolysaccharide group; A, A438079 group (an antagonist of P2X7 receptor); M, MCC950 group (an inhibitor of NLRP3); P, propofol group (a common hypnotic, 50 μM); P250, (250 μM); P500 (500 μM); I, intralipid group (vehicle of propofol)

Fig. 1c, in noncanonical pathway of pyroptosis, the expression of caspase-11 and P2X7R in the group L was higher than that in the group C (both $P < 0.001$). For apoptosis, LPS attack did not significantly change the expression of caspase-3 in cultured IEC-6 cells ($P > 0.05$ vs. group C; Fig. 1d).

Furthermore, the percentage of YO-PRO-1 stained cells was higher in the group L than that in the group C ($P < 0.001$; Fig. 2), indicating that the opening of P2X7R pore significantly increased after LPS challenge.

As shown in Fig. 3a, cytotoxicity in the group L were markedly higher than that in the group C ($P < 0.001$), indicating that the current LPS challenge led to increased pyroptosis in cultured cells. However, the molecules associated with canonical pyroptosis (IL-1β and IL-18) were not significantly different between two groups (both $P > 0.05$; Fig. 3b).

LPS Challenge Induced Activation of Caspase-11/P2X7R and Pyroptosis in Intestinal Epithelial Tissues, and Led to Intestinal Epithelial Injury and Mortality of Mice

In intestinal epithelia of animals, the expression of various molecules in canonical and noncanonical pathway of pyroptosis was also measured by western blot analysis (Fig. 4a). The expression of caspase-11 and P2X7R significantly elevated in the group L (both $P < 0.001$ vs. group C; Fig. 4c), whereas the expression of NLRP3, caspase-1 and caspase-3 was similar between the group C and group L (all $P > 0.05$; Fig. 4b, d), indicating that the

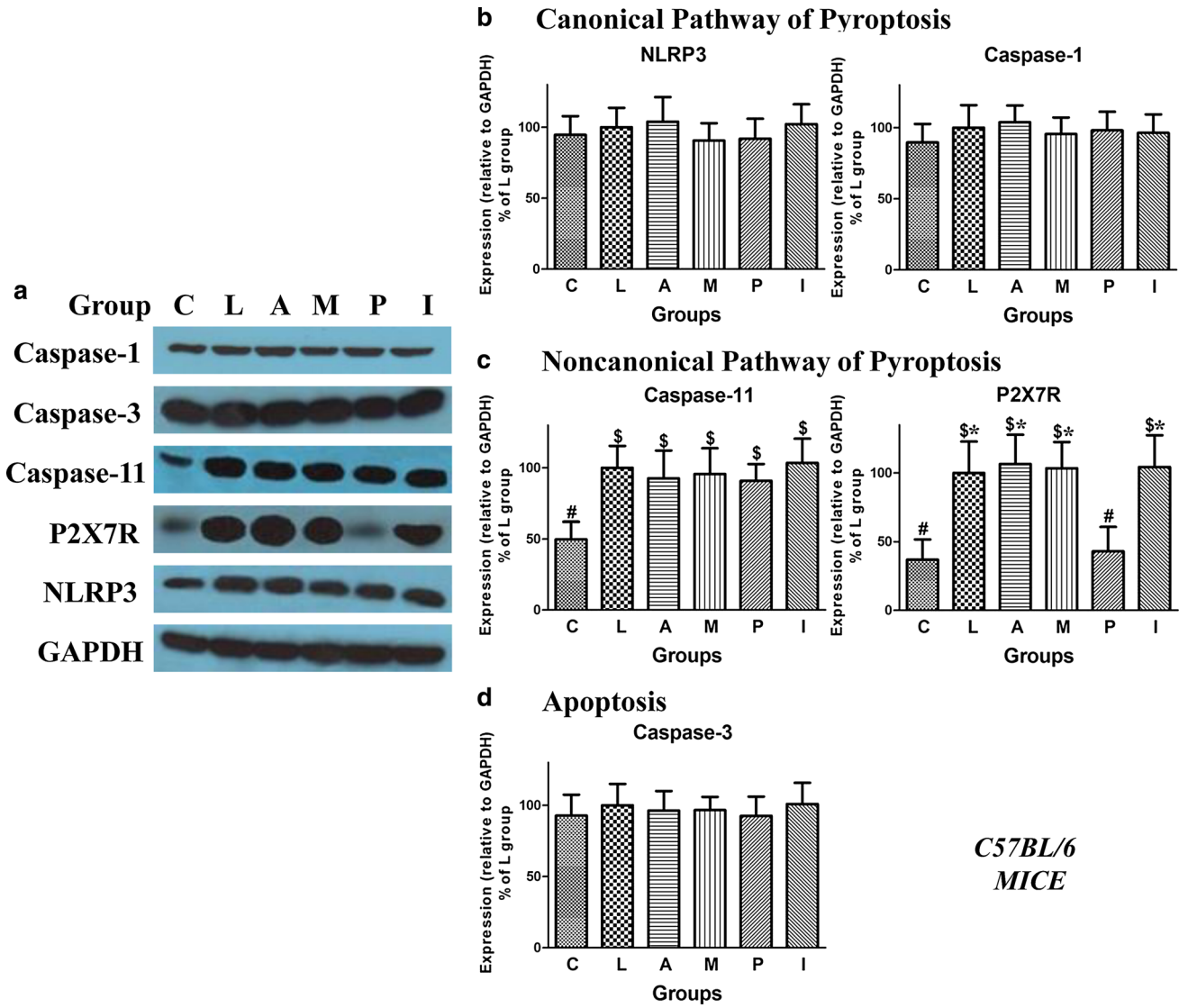

Fig. 4 Changes in the expression of various molecules in intestinal epithelia of mice. **a** The expression of various molecules in canonical and noncanonical pathways of pyroptosis was detected by western blot. Representative bands from densitometric analysis in experimental groups were presented. **b** The NLRP3 expression and caspase-1 expression in canonical pyroptosis were analyzed and presented. **c** The caspase-1 expression and P2X7R expression in noncanonical pyroptosis were analyzed and presented. **d** The caspase-3 expression was analyzed and presented. Data were expressed as mean ± SD, $n = 5$ or 6. Results were compared by ANOVA with Tukey posttest. $^{\$}P < 0.01$ versus the C group; $^{*}P < 0.01$ versus the P group; $^{\#}P < 0.01$ versus the L group. P2X7R, P2X7 receptor; C, control group; L, lipopolysaccharide group; A, A438079 group (a competitive antagonist of P2X7 receptor); M, MCC950 group (an inhibitor of NLRP3); P, propofol group (a common hypnotic, 50 mg/kg); I, intralipid group (vehicle of propofol)

current LPS regimen just activated noncanonical pyroptosis. As shown in Fig. 5, HMGB1, a biomarker of pyroptosis, in intestinal epithelial tissue was significantly higher in the group L ($P < 0.001$ vs. group C).

Moreover, higher Chiu's score and DAO concentration, and shorter villi were detected in the group L (all $P < 0.001$ vs. group C; Fig. 6), indicating that LPS attack led to severe intestinal epithelial injury. In survival analysis (Fig. 7), the survival time in the group L was 16 h (4–23 h), which was shorter than that in the group C ($P < 0.001$). In addition, the mortality rate was higher in the group L than that in the group C (100 vs. 0%; $P < 0.001$).

A438079, but Not MCC950 and Propofol, Reduced Enterocyte Pyroptosis, Intestinal Epithelial Injury and Mortality After LPS Challenge

In vitro, A438079, a competitive antagonist of P2X7R, did not significantly change the expression of P2X7R and the other molecules (all $P > 0.05$ vs. group L; Fig. 1). A438079 did not reduce the concentration of IL-1β, IL-18

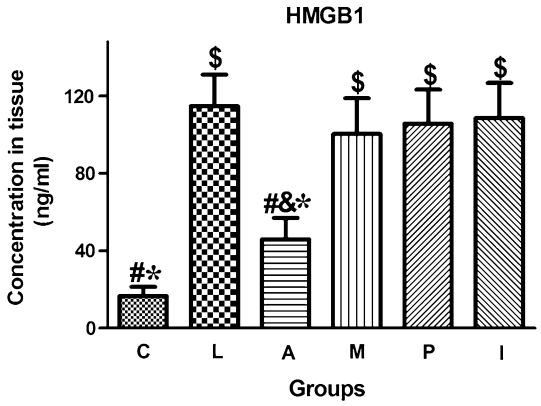

Fig. 5 Changes in HMGB1 concentration in mice's intestinal epithelial tissues. HMGB1 is an in vivo biomarker of pyroptosis. Thus, we examined HMGB1 concentration to evaluate the severity of pyroptosis in intestinal epithelia. The HMGB1 concentration was analyzed and presented. Data were expressed as mean ± SD, $n = 5$ or 6. Results were compared by ANOVA with Tukey posttest. $^{\&}P < 0.05$ versus the C group; $^{\$}P < 0.01$ versus the C group; $^{*}P < 0.01$ versus the *P* group; $^{\#}P < 0.01$ versus the L group. HMGB1, high-mobility group box-1 protein; C, control group; L, lipopolysaccharide group; A, A438079 group (an antagonist of P2X7 receptor); M, MCC950 group (an inhibitor of NLRP3); P, propofol group (a common hypnotic, 50 mg/kg); I, intralipid group (vehicle of propofol)

and ATP (Figs. 1b, 3b), but it decreased the percentage of YO-PRO-1 positive cells and cytotoxicity (both $P < 0.001$ vs. group L; Figs. 2, 3a), indicating that A438079 inhibited the opening of P2X7R and noncanonical pyroptosis.

In vivo, A438079 did not change P2X7R expression in epithelial tissues ($P > 0.05$ vs. group L; Fig. 4c), but it significantly reduced HMGB1 concentration in intestinal epithelia ($P = 0.04$ vs. group L; Fig. 5) and improved Chiu's score, DAO and villus length ($P = 0.002$, $P < 0.001$ and $P = 0.019$ vs. group L, respectively; Fig. 6). In survival analysis (Fig. 7), A438079 significantly prolonged survival time and reduced mortality ($P = 0.002$ and $P = 0.031$ vs. group L, respectively).

MCC950, a selective inhibitor of NLRP3, did not affect the expression of NLRP3, and it did not reduce pyroptosis of enterocyte and produce protective effects against LPS attack both in vitro and in vivo. (all $P > 0.05$ vs. group L; Figs. 1, 2, 3, 4, 5, 6, 7).

In our pilot experiment, propofol 50 μM decreased P2X7R expression in vitro. Thus, the concentration of propofol 50 μM was chosen. However, in the present study, propofol 50 μM did not reduce YO-PRO-1 uptake ($P > 0.05$ vs. group L; Fig. 2) and the concentration of IL-1β and IL-18 (both $P > 0.05$ vs. group L; Fig. 3b) although propofol 50 μM significantly decreased P2X7R expression ($P < 0.001$ vs. group L; Fig. 1c). Importantly, as shown in Fig. 3a, neither propofol 50 μM nor higher concentrations (250 μM and 500 μM) reduced cytotoxicity (all $P > 0.05$ vs. group L), indicating that propofol could not effectively inhibit enterocyte pyroptosis.

In vivo, propofol 50 mg/kg significantly decreased P2X7R expression in intestinal epithelia ($P = 0.001$ vs. group L; Fig. 4c), but it did not reduce HMGB1 concentration and intestinal epithelial injury (all $P > 0.05$ vs. group L; Figs. 5, 6). Furthermore, propofol 50 mg/kg did not improve survival time and mortality rate (both $P > 0.05$; Fig. 7).

Intralipid, vehicle of propofol, did not provide active effects both in vitro and in vivo (all $P > 0.05$ vs. group L; Figs. 1, 2, 3, 4, 5, 6, 7).

Discussion

The present results identify P2X7R-dependent enterocyte pyroptosis as a potential mechanism of gut barrier injury in sepsis and indicate that targeted treatments for pyroptosis should be developed.

Based on previous novel literatures [10, 17], a dual-LPS challenge was applied in this study, and it effectively induced caspase-11 and P2X7R activation in vitro and in vivo (Figs. 1c, 4c). Moreover, in line with Yang and Wu's results [10, 25], we found that the biomarkers of pyroptosis (cytotoxicity and HMGB1) significantly increased (Figs. 3, 5) after LPS attack. The current results indicate that, during sepsis, large amounts of LPS from the bacteria of gut lumen may activate caspase-11/P2X7R and subsequently cause pyroptosis of enterocytes. Previous studies mainly explored the role of pyroptosis of immune cells, such as macrophages and T subset cells, in the development of sepsis [10, 12, 20, 26]. To the best of our knowledge, our study, for the first time, discovers pyroptosis of intestinal epithelial cells in sepsis. Epithelial cells are critical for maintaining gut mucosal barrier. Therefore, in sepsis, pyroptosis of enterocytes induced by P2X7R activation probably leads to the disruption of intestinal epithelial structure. Interestingly, in this experiment, the caspase-3 and the molecules of canonical pyroptosis (NLRP3, caspase-1 and IL-1β/-18) were not activated (Figs. 1, 4). Several studies demonstrated that single LPS injection led to apoptosis of intestinal epithelial cells [27, 28] and NLRP3/caspase-1 activation in macrophages [29]. We suppose that the current dual-LPS regimen is prone to directly enhance intracellular LPS and then activate caspase-11/P2X7R pathway.

P2X7R plays a critical role in regulating canonical and noncanonical pyroptosis [10]. Several literatures demonstrated that P2X7R knockout attenuated sepsis-associated inflammation and mortality through maintaining immune responses [10, 12]. In this study, P2X7R expression significantly increased in cultured IEC-6 cells and in intestinal

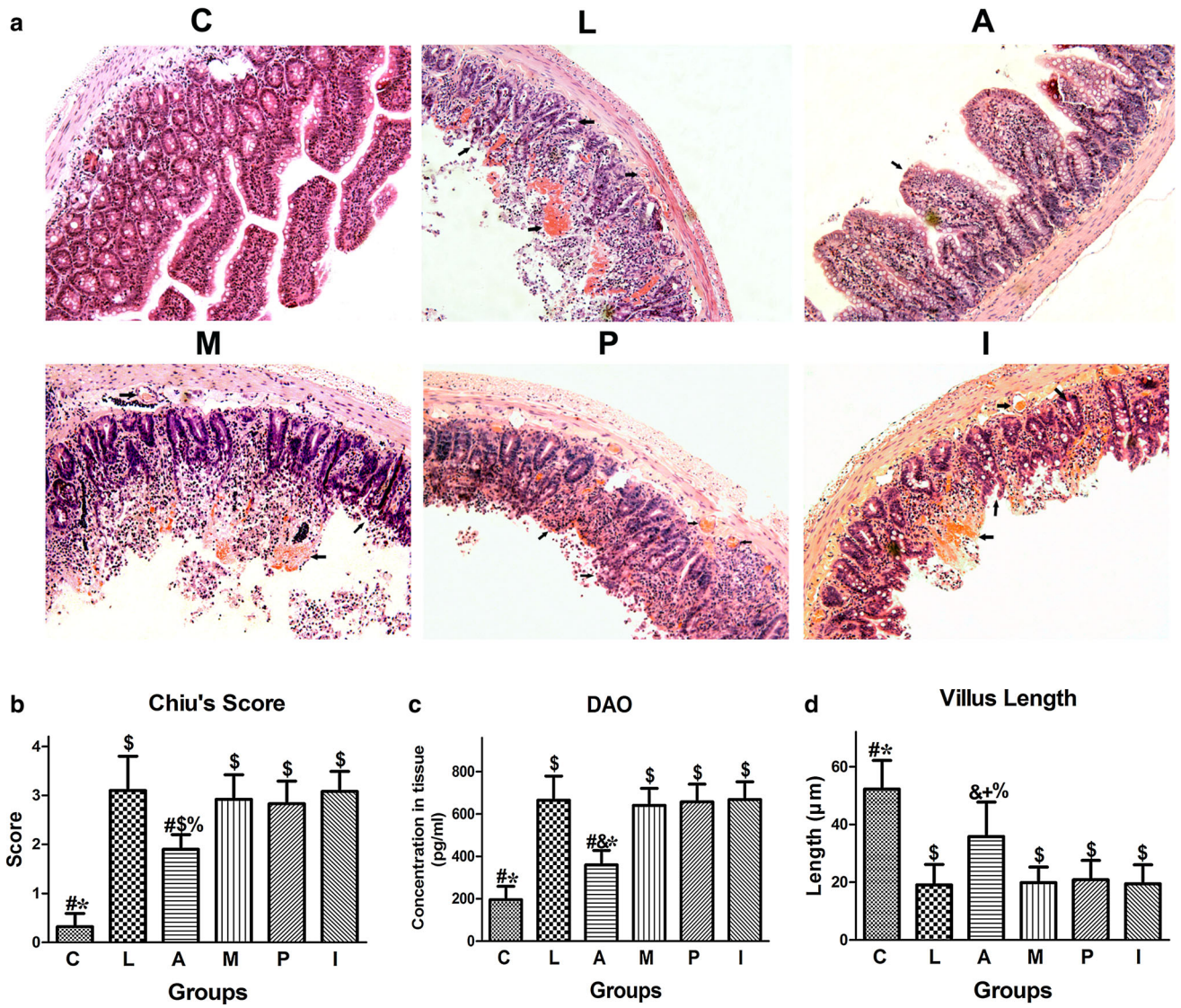

Fig. 6 Changes in intestinal epithelial injury of mice. **a** Representative microscopic images of ileal sections in experimental groups were shown. The intestinal sections were stained with hematoxylin–eosin and examined by light microscopy (×200). In the group C, normal structure of intestinal mucosa was seen. In contrast, in the group L, M, P and I, edema of villi, denuded villus tips and congested blood vessels were observed. Moreover, hemorrhage and sloughing of the epithelium were occasionally seen in several regions of intestinal specimens (black arrow). In the group A, mucosal structures were generally normal. However, blunt and short villi were frequently observed. **b** Change in Chiu's score is an indicator of gut histological damage. Chiu's score was analyzed and presented. **c** DAO is an indicator of the intestinal epithelial integrity and function. DAO concentration in supernatants of intestinal epithelia was analyzed and presented. **d** Villus length is another indicator of gut histological damage after sepsis. Villus length was analyzed and presented. Data were expressed as mean ± SD, $n = 5$ or 6. Results were compared by ANOVA with Tukey posttest. $^{\&}P < 0.05$ versus the C group; $^{\$}P < 0.01$ versus the C group; $^{\%}P < 0.05$ versus the P group; $^{*}P < 0.01$ versus the P group; $^{+}P < 0.05$ versus the L group; $^{\#}P < 0.01$ versus the L group. DAO, diamine oxidase; C, control group; L, lipopolysaccharide group; A, A438079 group (an antagonist of P2X7 receptor); M, MCC950 group (an inhibitor of NLRP3); P, propofol group (a common hypnotic, 50 mg/kg); I, intralipid group (vehicle of propofol)

epithelia of mice following LPS challenge. A438079, a competitive and specific antagonist of P2X7R, decreased pyroptosis of enterocytes in vitro and in vivo (Figs. 3, 5) and then ameliorated intestinal epithelial injury and mortality of mice (Figs. 6, 7), indicating that blocking of P2X7R may be an effective way to reduce pyroptosis-induced gut barrier injury and death during sepsis. MCC950 is a potent and selective inhibitor of NLRP3, and it blocks NLRP3-dependent pyroptosis induced by extracellular LPS [30], whereas because the current LPS regimen induced pyroptosis independently of NLRP3, MCC950 could not relieve enterocyte pyroptosis in this study. Our results support the notion that P2X7R is a promising therapeutic target against sepsis-induced intestinal epithelial disruption

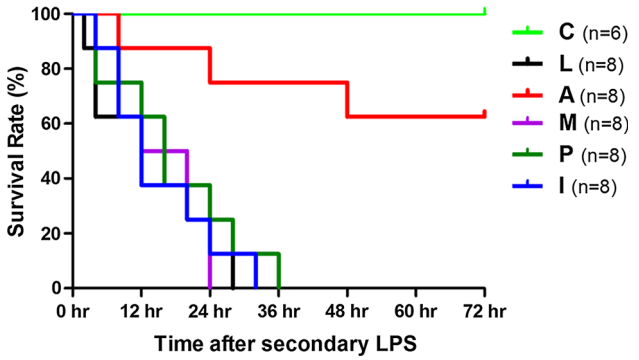

Fig. 7 Survival analysis within 72 h after LPS challenge. The independent mice underwent different interventions based on the current experimental protocol. Survival time was calculated from the secondary injection of LPS, $n = 6$–8. Results were compared by Kaplan–Meier log-rank test and Fisher's exact test. The mice in the group L succumbed within 30 h. Survival time and mortality rate in the group A were significantly improved, whereas, survival times in the group P, M and I were not prolonged. LPS, lipopolysaccharide; C, control group; L, lipopolysaccharide group; A, A438079 group (an antagonist of P2X7 receptor); M, MCC950 group (an inhibitor of NLRP3); P, propofol group (a common hypnotic, 50 mg/kg); I, intralipid group (vehicle of propofol)

and septic diseases. However, the role of P2X7R in sepsis is still controversial. Csóka and Proietti et al. suggested that, in sepsis, P2X7R promotes host-microbiota mutualism, and activation of P2X7R conferred the protection through enhancing bacterial killing capacity of immune antibodies and cells [20, 26]. Therefore, further studies are necessary to address the modulation of P2X7 expression and function at different stages of sepsis.

Recent studies reported that several synthetic proteins reduced pyroptosis of macrophage and organic injury by inhibiting the expression and action of P2X7R [31, 32]. Propofol is widely used for sedation in septic patients in the clinical settings. In this study, we found that propofol significantly decreased P2X7R expression in intestinal epithelial cells (Figs. 1c, 4c), but propofol relieved neither enterocyte pyroptosis nor intestinal epithelial injury after LPS challenge (Figs. 3, 5). Yang et al. [10] indicated that cytosolic LPS markedly increased the sensitivity of the P2X7R-associated pore and pyroptosis to ATP stimulation. Thus, one possibility was that P2X7 receptors were sensitized and opened by increased cytosolic LPS (caspase-11 activation) and extracellular ATP (Fig. 1b) following LPS attack; the present propofol concentration was not able to adequately block the opening of P2X7R pores and the uptake of large molecules and water (Fig. 2) although it inhibited partial P2X7R expression. Indeed, Liu et al. [33] found that, in clinically relevant concentrations, propofol increased the current amplitudes through single P2X7R pore in cultured astrocytes. Due to a classical conversion of drug doses from animal to human [34], propofol 50 mg/kg in mouse is equal to approximately 5.5 mg/kg in human. This dose of propofol far exceeded the usual dosage in clinical practice yet still failed to alleviate LPS-induced pyroptosis (Fig. 5), intestinal epithelial disruption (Fig. 6) and animal's death (Fig. 7). Previous studies suggested that propofol was a preferential sedative drug for septic patients because propofol inhibited enterocyte apoptosis [14]. However, our data demonstrated that propofol provided no protection against enterocyte pyroptosis mediated by caspase-11/P2X7R, and therefore, an additional therapy for pyroptosis should be developed.

There were several limitations in the present study. First, the current LPS regimen did not activate canonical pyroptosis and apoptosis of enterocytes. In further researches, classic sepsis models, including CLP and bacterial infection, should be applied to explore the effect of propofol on pyroptosis and even other programmed cell death. However, our results have indicated that propofol conferred no protection for LPS-induced pyroptosis. Second, unfortunately, the specific in vivo biomarkers of pyroptosis are still absent [21]. The increased HMGB1 levels may reflect necrosis or activation of macrophages. However, the upregulation of caspase-11 and P2X7R in mice's intestinal epithelia strongly indicated that the release of HMGB1 was mainly caused by enterocyte pyroptosis. Third, our data suggested that P2X7R played an important role in enterocyte pyroptosis after LPS attack. However, appropriate models of P2X7R signaling, such as P2X7R or caspase-11 null, should be applied to clarify the correlation between enterocyte pyroptosis and caspase-11/P2X7R expression, and to provide depth mechanistic insight of P2X7R in sepsis-induced intestinal epithelial injury.

In summary, LPS challenge leads to activation of caspase-11 and P2X7R, and subsequent pyroptosis of enterocyte in cultured cells and intestinal epithelia. Antagonizing P2X7R by specific antagonist reduces enterocyte pyroptosis and intestinal epithelial injury, as well as mortality, following LPS attack. Propofol does not improve enterocyte pyroptosis and death of mice, although it effectively inhibits P2X7R expression. Our study provides new insights into the mechanism of sepsis development and exhibits the potential therapeutic approach for sepsis-induced intestinal injury.

Acknowledgments The authors thank Yi-Hong Ling M.D. and Yuan-Zhong Yang M.D. (Department of Pathology, Sun Yat-sen University Cancer Center, Guangdong, China) for their in histological analysis. The authors thank Dr. Jie Li (Laboratory Animal Center, Sun Yat-sen University) for her help in animal experiments.

Funding The present study was supported by grants from the Natural Science Foundation of Guangdong Province, China (Grant No. 2014A030313210 to Zi-Meng Liu).

Compliance with ethical standards

Conflict of interest The authors declare that they have no conflict of interest.

References

1. Mira JC, Gentile LF, Mathias BJ, et al. Sepsis pathophysiology, chronic critical illness, and persistent inflammation-immunosuppression and catabolism syndrome. *Crit Care Med*. 2017;45:253–262.
2. Stoller J, Halpin L, Weis M, et al. Epidemiology of severe sepsis: 2008–2012. *J Crit Care*. 2016;31:58–62.
3. Yoseph BP, Klingensmith NJ, Liang Z, et al. Mechanisms of intestinal barrier dysfunction in sepsis. *Shock*. 2016;46:52–59.
4. Derikx JP, Poeze M, van Bijnen AA, Buurman WA, Heineman E. Evidence for intestinal and liver epithelial cell injury in the early phase of sepsis. *Shock*. 2007;28:544–548.
5. Chawla LS, Fink M, Goldstein SL, et al. The epithelium as a target in sepsis. *Shock*. 2016;45:249–258.
6. Wu R, Dong W, Qiang X, et al. Orexigenic hormone ghrelin ameliorates gut barrier dysfunction in sepsis in rats. *Crit Care Med*. 2009;37:2421–2426.
7. Li Z, Zhang X, Zhou H, Liu W, Li J. Exogenous *S*-nitrosoglutathione attenuates inflammatory response and intestinal epithelial barrier injury in endotoxemic rats. *J Trauma Acute Care Surg*. 2016;80:977–984.
8. Coopersmith CM, Stromberg PE, Dunne WM, et al. Inhibition of intestinal epithelial apoptosis and survival in a murine model of pneumonia-induced sepsis. *JAMA*. 2002;287:1716–1721.
9. Li MX, Liu JF, Lu JD, et al. Plasmadiafiltration ameliorating gut mucosal barrier dysfunction and improving survival in porcine sepsis models. *Intensive Care Med Exp*. 2016;4:31.
10. Yang D, He Y, Muñoz-Planillo R, Liu Q, Núñez G. Caspase-11 requires the Pannexin-1 channel and the Purinergic P2X7 pore to mediate pyroptosis and endotoxic shock. *Immunity*. 2015;43:923–932.
11. Jorgensen I, Miao EA. Pyroptotic cell death defends against intracellular pathogens. *Immunol Rev*. 2015;265:130–142.
12. Santana PT, Benjamim CF, Martinez CG, Kurtenbach E, Takiya CM, Coutinho-Silva R. The P2X7 receptor contributes to the development of the exacerbated inflammatory response associated with sepsis. *J Innate Immun*. 2015;7:417–427.
13. Bilodeau MS, Arguin G, Gendron FP. C/EBPβ regulates P2X7 receptor expression in response to glucose challenge in intestinal epithelial cells. *Biochem Cell Biol*. 2015;93:38–46.
14. Tang J, Jiang Y, Tang Y, et al. Effects of propofol on damage of rat intestinal epithelial cells induced by heat stress and lipopolysaccharides. *Braz J Med Biol Res*. 2013;46:507–512.
15. Yagmurdur H, Aksoy M, Arslan M, Baltaci B. The effects of propofol and ketamine on gut mucosal epithelial apoptosis in rats after burn injury. *Eur J Anaesthesiol*. 2007;24:46–52.
16. Wang W, Lu R, Feng DY, Liang LR, Liu B, Zhang H. Inhibition of microglial activation contributes to propofol-induced protection against post-cardiac arrest brain injury in rats. *J Neurochem*. 2015;134:892–903.
17. Hagar JA, Powell DA, Aachoui Y, Ernst RK, Miao EA. Cytoplasmic LPS activates caspase-11: implications in TLR4-independent endotoxic shock. *Science*. 2013;341:1250–1253.
18. Zhang XY, Liu ZM, Zhang HF, et al. TGF-β1 improves mucosal IgA dysfunction and dysbiosis following intestinal ischaemia-reperfusion in mice. *J Cell Mol Med*. 2016;20:1014–1023.
19. He WT, Wan H, Hu L, et al. Gasdermin D is an executor of pyroptosis and required for interleukin-1β secretion. *Cell Res*. 2015;25:1285–1298.
20. Csóka B, Németh ZH, Törő G, et al. Extracellular ATP protects against sepsis through macrophage P2X7 purinergic receptors by enhancing intracellular bacterial killing. *FASEB J*. 2015;29:3626–3637.
21. Demon D, Kuchmiy A, Fossoul A, Zhu Q, Kanneganti TD, Lamkanfi M. Caspase-11 is expressed in the colonic mucosa and protects against dextran sodium sulfate-induced colitis. *Mucosal Immunol*. 2014;7:1480–1491.
22. Wolvekamp MC, de Bruin RW. Diamine oxidase: an overview of historical, biochemical and functional aspects. *Dig Dis*. 1994;12:2–14.
23. Liew VY, Chapman MJ, Nguyen NQ, et al. A prospective observational study of the effect of critical illness on ultrastructural and microscopic morphology of duodenal mucosa. *Crit Care Resusc*. 2016;18:102–108.
24. Dominguez JA, Samocha AJ, Liang Z, Burd EM, Farris AB, Coopersmith CM. Inhibition of IKKβ in enterocytes exacerbates sepsis-induced intestinal injury and worsens mortality. *Crit Care Med*. 2013;41:e275–e285.
25. Wu D, Pan P, Su X, et al. Interferon regulatory factor-1 mediates alveolar macrophage pyroptosis during LPS-induced acute lung injury in mice. *Shock*. 2016;46:329–338.
26. Proietti M, Cornacchione V, Rezzonico Jost T, et al. ATP-gated ionotropic P2X7 receptor controls follicular T helper cell numbers in Peyer's patches to promote host-microbiota mutualism. *Immunity*. 2014;41:789–801.
27. Yue C, Wang W, Tian WL, et al. Lipopolysaccharide-induced failure of the gut barrier is site-specific and inhibitable by growth hormone. *Inflamm Res*. 2013;62:407–415.
28. Song D, Zong X, Zhang H, et al. Antimicrobial peptide cathelicidin-BF prevents intestinal barrier dysfunction in a mouse model of endotoxemia. *Int Immunopharmacol*. 2015;25:141–147.
29. Chen X, Wang N, Zhu Y, Lu Y, Liu X, Zheng J. The antimalarial chloroquine suppresses LPS-induced NLRP3 inflammasome activation and confers protection against murine endotoxic shock. *Mediators Inflamm*. 2017;2017:6543237.
30. Coll RC, Robertson AA, Chae JJ, et al. A small-molecule inhibitor of the NLRP3 inflammasome for the treatment of inflammatory diseases. *Nat Med*. 2015;21:248–255.
31. Dela Cruz CS, Liu W, He CH, et al. Chitinase 3-like-1 promotes *Streptococcus pneumoniae* killing and augments host tolerance to lung antibacterial responses. *Cell Host Microbe*. 2012;12:34–46.
32. Hu Z, Murakami T, Suzuki K, et al. Antimicrobial cathelicidin peptide LL-37 inhibits the LPS/ATP-induced pyroptosis of macrophages by dual mechanism. *PLoS One*. 2014;9:e85765.
33. Liu J, Gao XF, Ni W, Li JB. Effects of propofol on P2X7 receptors and the secretion of tumor necrosis factor-α in cultured astrocytes. *Clin Exp Med*. 2012;12:31–37.
34. Reagan-Shaw S, Nihal M, Ahmad N. Dose translation from animal to human studies revisited. *FASEB J*. 2008;22:659–661.